International Journal for Multidisciplinary Research (IJFMR)
E-ISSN: 2582-2160 ● Website: www.ijfmr.com ● Email: editor@ijfmr.com

Analytical Modeling of Electrical Frequency and Voltage Signal from a Differential Inductive Transduction for Energy Measurement

Abdulwahab Deji[1], Sheroz Khan[2], Musse Mohamoud Ahmad[3]

[1]Department of Electrical Computer Information and Telecommunication Engineering, Waidsum University Malaysia.
[2]Department of Electrical Engineering Onaizah College Saudi Arabia.
[3]Department of Electrical and Computer Engineering University of Malaysia Sarawak.

Abstract
This paper demonstrates a modeling of a frequency signal using inductive sensing mechanism in finding utility in vibration/oscillation circuits thereby converting deflections in milli and micro variance into useful frequency signal. It is a novel approach of an inductive sensor based on the basic principle of producing inductive changes in proportion to vibration deflections in a differential inductive coupling. Thus, enabling data management of the resultingoscillation applications in a real-time implementation. This circuit does not only detect and optimizes the deflections produced in an oscillation in instrumentation electronics, but also provide an improved sensory with high accuracy, sensitivity, responsiveness and operating range. The design therefore helps in transforming the deflection deviations in the inward and outward movement of the core into useful output content. A simulation and derivation of the oscillating circuit in see-saw convulsion bar sensing system has been implemented. Simulation and derivations show how the oscillating circuits of the bar are converted into frequency, current, voltages for further wireless applications. This is a pressure sensor which can be used for the acquisition of cardiovascular data into signal, and it's proven to be very helpful in diagnostic procedures.

Keywords: Differential inductive sensing, displacement inductance-to-frequency converter, deflection deviation, see-saw bar, oscillation, position sensing, cardiovascular data, inductive sensing, pressure sensor.

1. Introduction

Sensors have proven important in converting immeasurable quantities such as wind velocity, vibrations, oscillation, turning effects of forces, deviations, illness, temperature etc into continuous and discrete electrical signal suitable for real time implementation using smart oscillation harvesting mechanism. For an accurate measurement of such oscillation parameter, an efficient oscillation detector is unarguably paramount. These kinds of smart devices can be designed using an inductive coupling. The sensing in this case is a function of the displacement of the core brought about by the deflection when the device oscillates. This is capable of converting a see-saw convulsion bar into frequency response, duty cycle response, voltage response. The sensor outputshould be such that the oscillation/vibration, their motion,

damping etc is determined. Based on the sensing inductive principle used, the designed circuit can be categorized into a vibration sensor

and pressure sensor applied even in height location such as; sagging and oscillations of electrical transmission line, turning moment in railroad, signal upgrade from degradation in GSM mask [1]-[4]. The sensor output should be such that electro-mechanical deviations in oscillation circuit andtheir effects servomechanism are determined. The vibration sensor can be categorized according to the sensing element such as resistive, capacitive, inductive and linear variable differential transducer [5]-[6]. Piezo-resistive sensors have good linearity and acceptable sensitivity, but sufferfrom the problem of inaccuracies [7]-[8]. Capacitive pressure/oscillation sensors exhibit features of higher sensitivity and lower temperature hysteresis, but they are usually nonlinear [8-10]. Conventional LVDT-based pressure/oscillation sensors possess good linearity, highest sensitivityand lowest temperature hysteresis, but such devices have got bulky physical structures [9]-[12]. This paper presents a sensor capable of harnessing oscillations in circuits into pulse able signal. Each aspect of this finding has been put into different sections. Section I gives the introduction, section II describes the novel structural model and design, section III describes the theoretical background, derivation technique. Results from simulations and analysis are given in section IV; while conclusion is presented in section V. A simple modeling is shown in Figure 1.

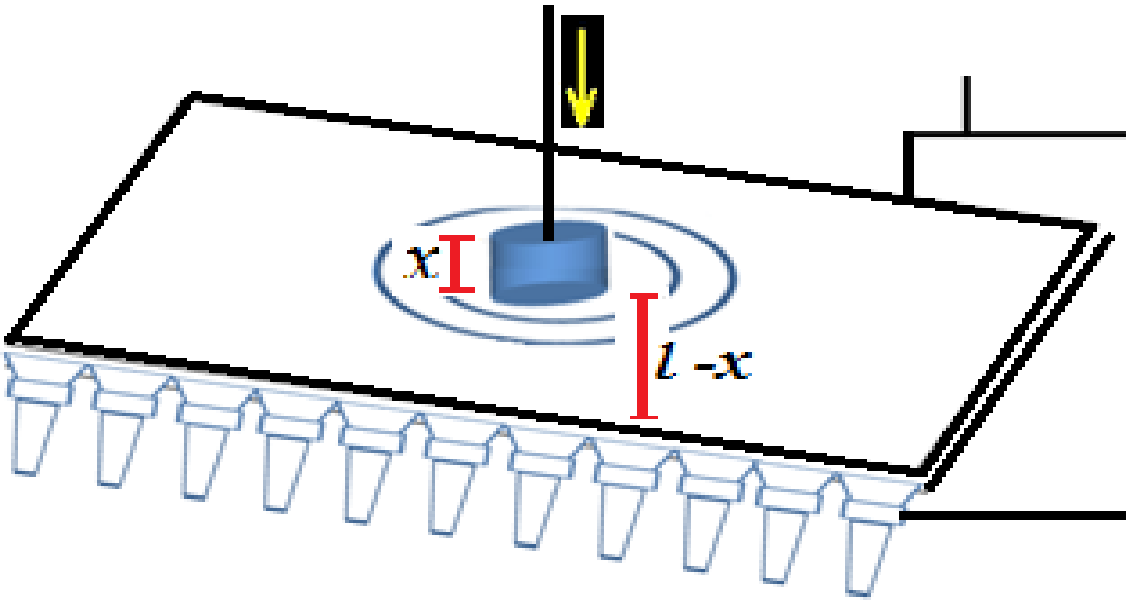

(a)

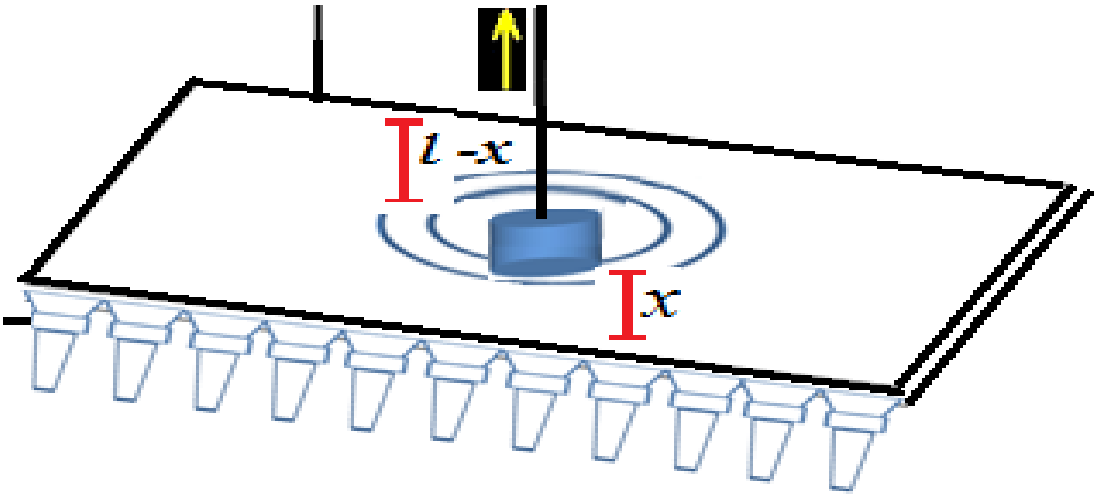

(b)

Figure 1 (a) Differential core moving into a coil due to vibrations (b) Differential core moving out of the coil due to vibrations

2. Design Model

The structure of the proposed oscillating circuit is shown schematically in Figure 2. The oscillationof the actual component of the sensor varying differentially, maximizing the circuit variations anddeviations into a derivable and pulse able signal is shown in Figure 3. As shown in Figure 2, 3and4, a vertical core of a varying height of 4mm to 36mm is embedded into an open stator made up of magnetic coils thereby providing the inductive change in relation to circuit vibrations. The oscillation of the circuit provides the force or pressure needed to bring about the inductance of thecoil as the core is displaced in and out of the coils mounted in a stator of a servomechanism. Thisdisplacement is proportional to the force or pressure and the inductance of the core. This is capable of converting a see-saw convulsion bar into frequency response, duty cycle response, voltage response. The sensor output should be such that the oscillation/vibration, their motion, damping etc is determined. Based on the sensing inductive principle used, the designed circuit can be categorized into a vibration sensor and pressure sensor applied even in height location such as; sagging and oscillations of electrical transmission line, turning moment in railroad, signal upgrade from degradation in GSM mask [1]-[4]. The sensor output should be suchthat electro-mechanical deviations in oscillation circuit and their effects servomechanism are determined. The vibration sensor can be categorized according to the sensing element such as resistive, capacitive, inductive and linear variable differential transducer [5]-[6]. Piezo-resistive sensors have good linearity and acceptable sensitivity, but suffer from the problem of inaccuracies [7]-[8]. Capacitive pressure/oscillation sensors exhibit features of higher sensitivity and lower temperature hysteresis, but they are usually nonlinear [8-10]. Conventional LVDT-based pressure/oscillation sensors possess good linearity, highest sensitivity and lowest temperature hysteresis, but such devices have got bulky physical structures [9]-[12]. This paper presents a sensor capable of harnessing oscillations in circuits into pulse able signal. Each aspect of this finding has been put into different sections. Section I gives the introduction, section II describes the novel structural model and design, section III describes the theoretical background, derivationtechnique. Results from simulations and analysis are given in section IV; while conclusion is presented in section V.

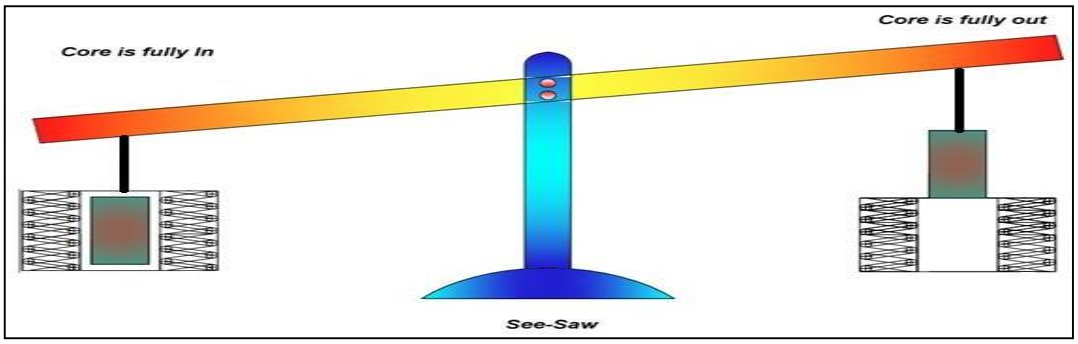

Figure 2. Varying differential cores in a see-saw

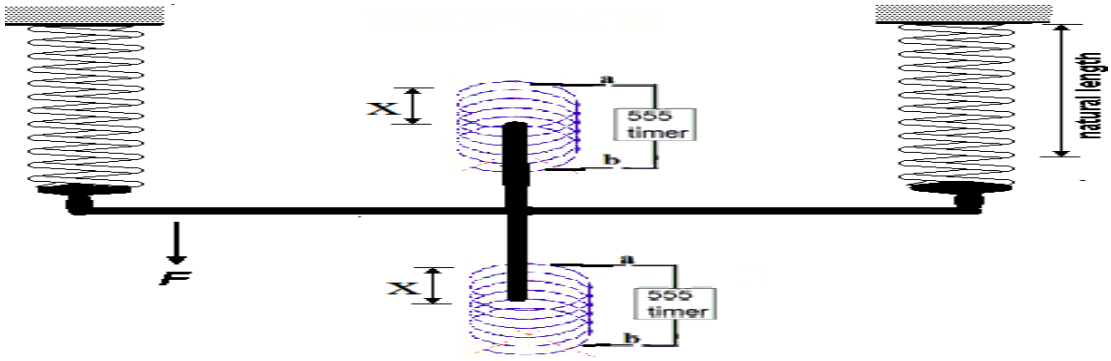

Figure 3. Signal produced from circuit oscillation and vibrations.

The timer circuit when connected to the coils in Figure 1 and Figure 2 will give rise to Figure 4. This RL3R circuit gives us a square wave with a frequency depending on the inductance value ofthe coil as shown in Figure 4.

The output voltage from the timer which shows the high and low time period that gives the duty cycle is given in Figure 4

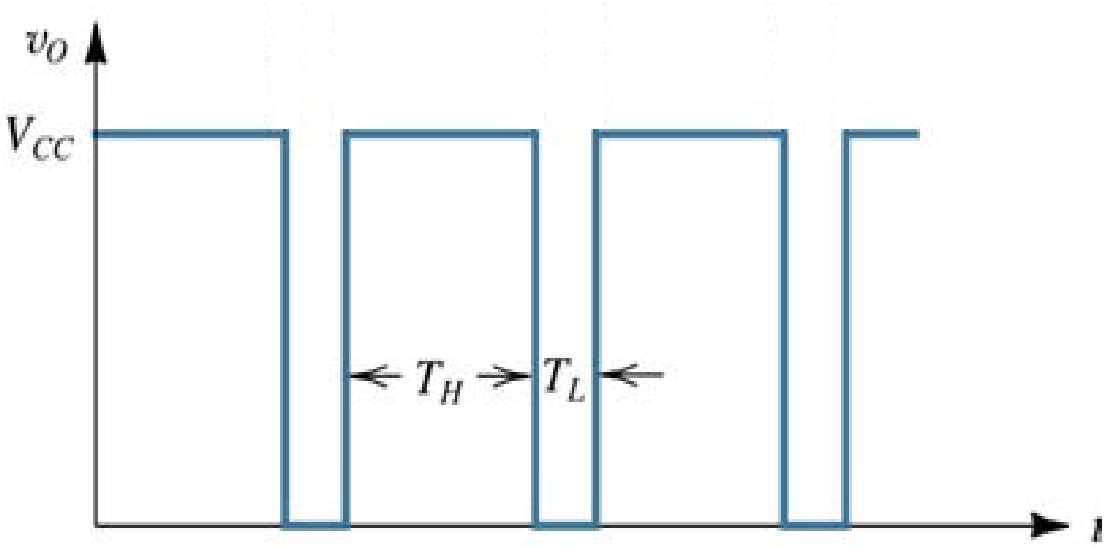

Figure Error! No text of specified style in document**..1 Output Voltage from timer.**

Figure 4. Voltage waveform from circuit Oscillation

3. Mathematical Model of the Circuit

A differential transducer is one that simultaneously senses two separate sources and provides an output proportional to the difference between the sensing. Considering the idea in Figure 4, the inductances of the two coils change in a differential manner when the overhanging bar is moving in a seesaw manner. At position '*x*', the inductance of the right hand side of the coil is given by Equation. (1), while that of the left hand side is given by Equation. (2), giving the total equation as follows:

$$L_{TOTAL} = \frac{\mu_0 N^2 A}{l}\left[\mu_r \frac{x}{l} + \frac{l-x}{l}\right] = \frac{\mu_0 N^2 A}{l}\left[1 + \frac{x}{l}(\mu_r - 1)\right] \quad (1)$$

$$L_{TOTAL} = \frac{\mu_0 N^2 A}{l}\left[\frac{x}{l} + \mu_r\left(\frac{l-x}{l}\right)\right] = \frac{\mu_0 N^2 A}{l}\left[\mu_r + \frac{x}{l}(1-\mu_r)\right] \quad (2)$$

Details of the derivation of equation 1 and 2 are shown in the APPENDIX A-1 to A-6.

A linear relationship is shown in Fig. 6 demonstrating the in and out oscillation of the device.

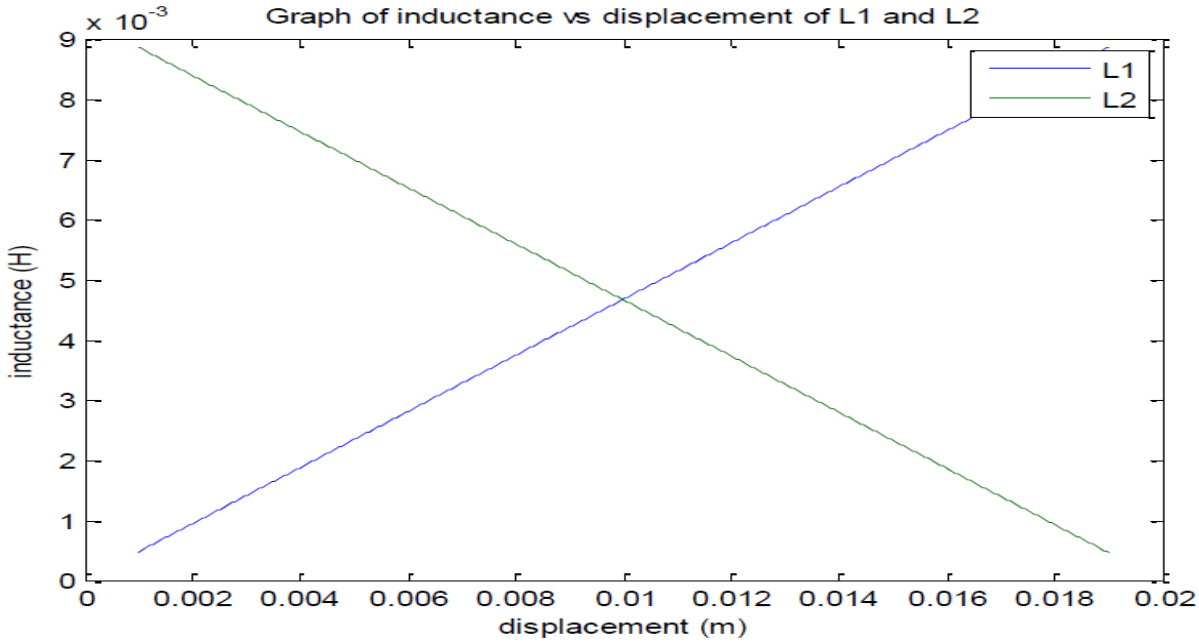

Figure 6 Inductive change with displacement

3.1 Frequency Output for Inductive change delta L

The frequency of RL3R-timer circuit for single inductor is given by:

$$f = 1.58\frac{R}{L}$$

The frequency of the first inductor is:

$$f_1 = 1.58\frac{R}{Lfi - \Delta L1} \quad (3)$$

The frequency of the second inductor is:

$$f_2 = 1.58\frac{R}{Lfo + \Delta L2} \quad (4)$$

The frequency of total inductive change is:

$$\Delta f_1 = f_1 - f_{fi} = 1.58\,R\left(\frac{1}{L_1} - \frac{1}{L_{fi}}\right) \quad (5)$$

Substituting the value of L_1 in equation (5) we get:

$$\Delta f_1 = 1.58\,R\left(\frac{\Delta L1}{(Lfi - \Delta L1)\,L_{fi}}\right) \quad (6)$$

Now solving for the other case of Δf_2, we obtain;

$$\Delta f_2 = f_{fo} - f_2 = 1.58\, R\left(\frac{1}{L_{f0}} - \frac{1}{L_2}\right) \quad (7)$$

Hence,

$$\Delta f_2 = 1.58\, R\left(\frac{\Delta L1}{(Lfi - \Delta L1)\, L_{fi}}\right) \quad (8)$$

$$\Delta f_{avr} = \frac{\Delta L1 + \Delta L2}{2} \quad (9)$$

3.2 Frequency change as a function of displacement

From the previous equation, the frequency change as a function of displacement is given thus as:

$$\Delta f_1 = 1.58\, R\left(\frac{l^2}{\mu_0 N^2 A(l + x(\mu_r - 1))} - \frac{1}{L_{fi}}\right) \quad (10)$$

That of the second coil is;

$$\Delta f_2 = 1.58\, R\left(\frac{1}{L_{f0}} - \frac{l^2}{\mu_0 N^2 A(\mu_r\, l + x(1 - \mu_r))}\right) \quad (11)$$

The plot for frequencies of the in and out movement of the core in the coil is given as;
These change in frequencies from equations [11] and [12], gives a symmetrical behaviour with respect to the displacement produced by the oscillatory motion of the core. This aforementioned behaviour gave rise the plot in Figure 7 (a) showing the reciprocal behaviour of the in and out movement, harnessing the deviations in terms of oscillation in servomechanism and electro-mechanical devices.

3.3 Frequency response from displacement

The result from the position sensor as analytically obtained in equation 10 and 11. This shows the behavior in response when the output frequency from the different magnetic core materials such as iron, nickel and copper is when plotted against the displacement provided by the wind, force, thereby causing oscillation resulting to this inward and outward movement of the core in coil geometry. These responses for this different kind of materials are shown in Figure 7.

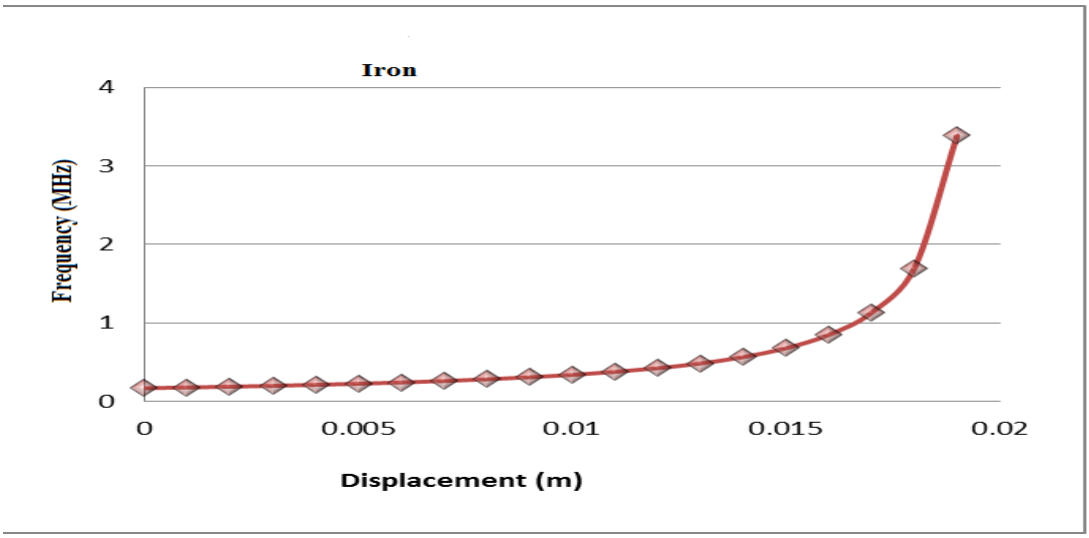

(a)

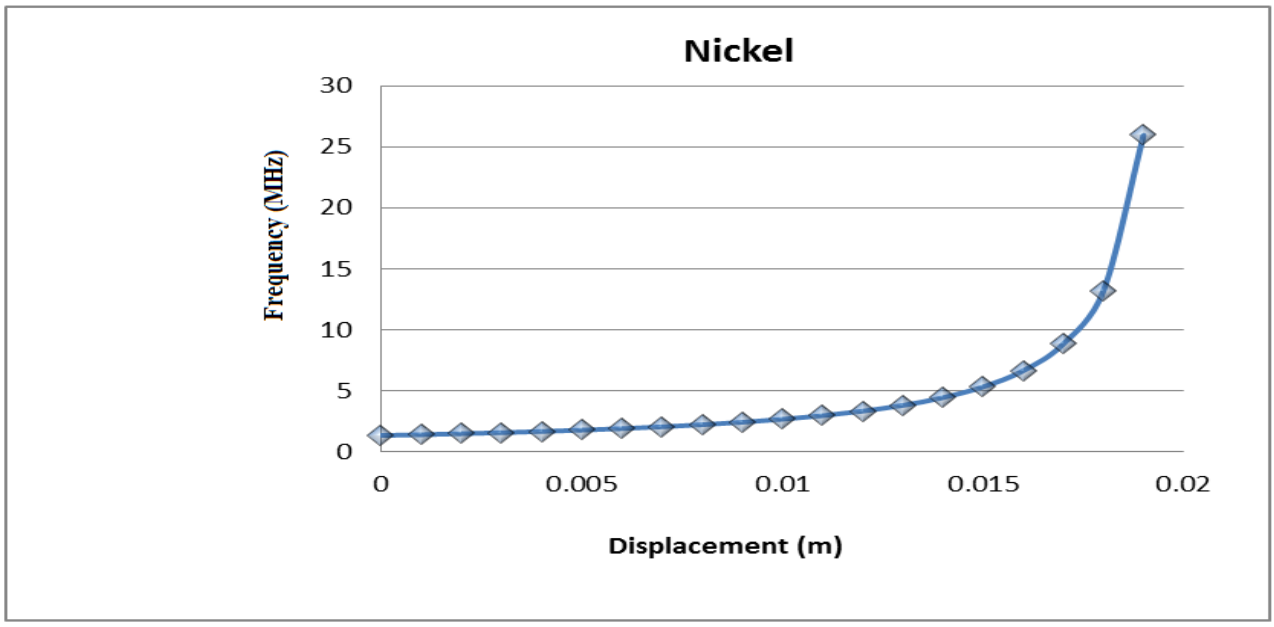

(b)

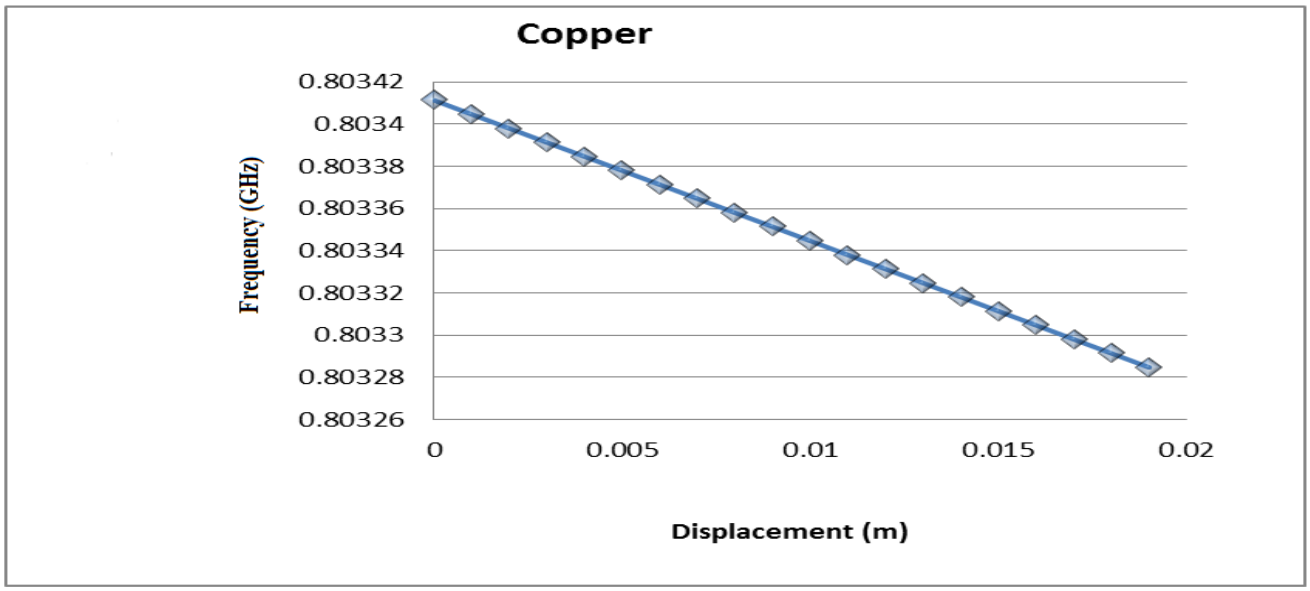

(c)

Figure 7 (a-c) shows frequency response for iron, nickel and copper.

The frequency as a result of differential displacement of the core is shown in Figure 8

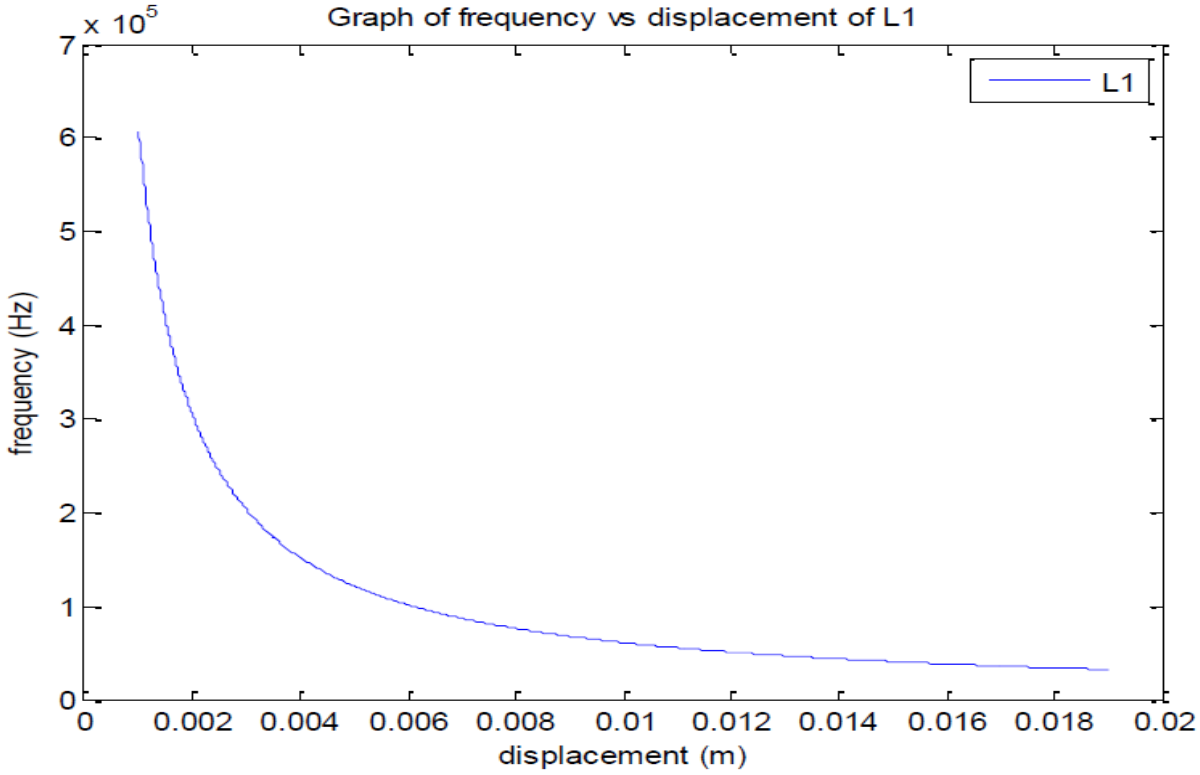

(a)

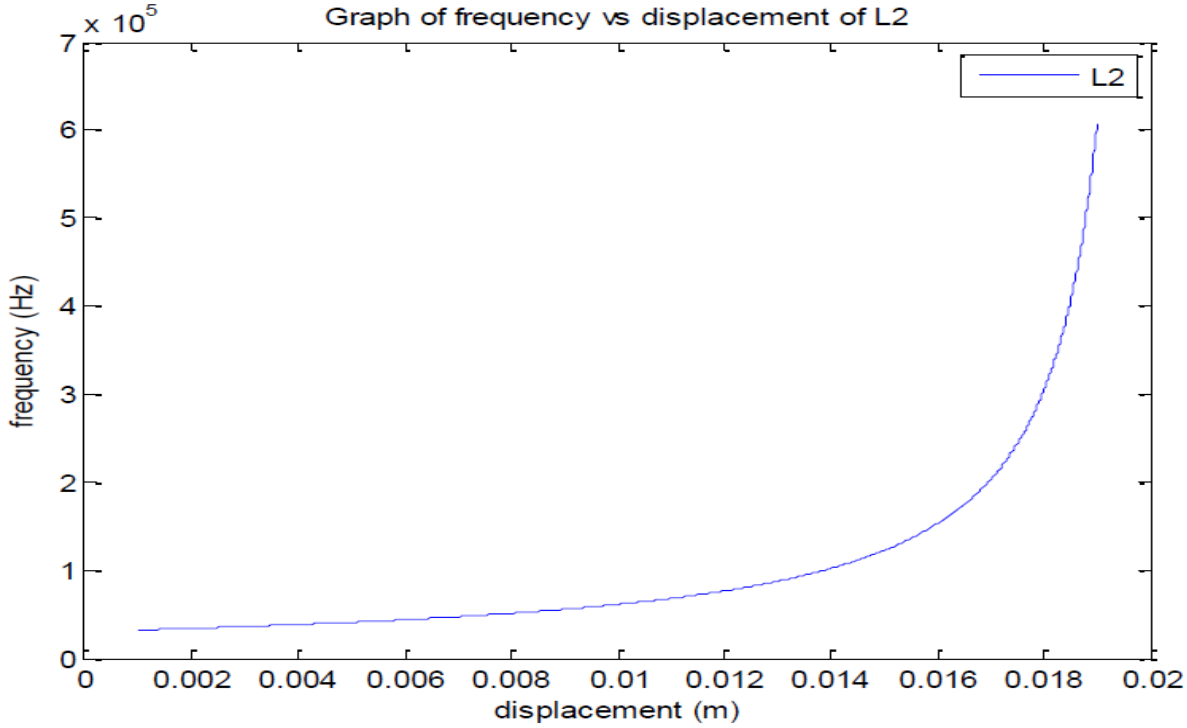

(b)

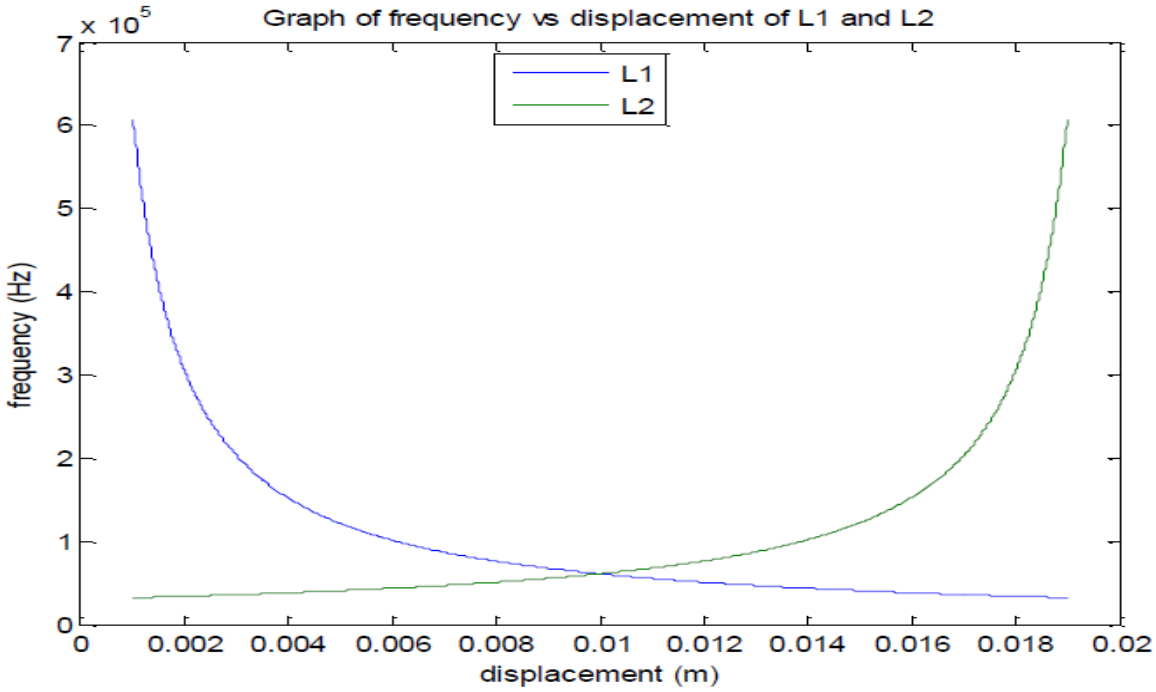

(c)

Figure 8 (a-c) Frequency as a result of differential displacement of the core

The range of the output frequency is very high in paramagnetic materials (nickel) than in ferromagnetic material (iron), while there is an inverse output frequency for diamagnetic material (copper). Hence, the designed circuit is used to characterize the type of materials that could be used in some specific applications.

Assuming a coil of length of 20mm, number of turns = 100, cross sectional area A=pi(r*r) where r=1mm, and R=1k ohm

1. Iron core with relative permeability 4728
2. Nickel core with relative permeability 600.
3. Copper core with relative permeability 0.999834.

The result from the frequency output for iron core, nickel core and copper core are shown in table 1

Table 1: Displacement with Firon,, Fnickel and Fcopper

X (m)	f Iron (KHz)	f nickel (MHz)	f copper (MHz)
0	169898.06	1338796.71	803411389.7
0.001	178838.07	1409136.08	803404720.4
0.002	188771.18	1487276.47	803398051.1
0.003	199872.61	1574591.83	803391382
0.004	212361.34	1672798.88	803384712.9
0.005	226514.78	1784071.12	803378044
0.006	242689.51	1911201.58	803371375.2
0.007	261351.86	2057840.46	803364706.5
0.008	283123.51	2228851.34	803358037.9
0.009	308852.12	2430861.02	803351369.4

0.01	339724.26	2673138.18	803344701.1
0.011	377453.67	2969055.71	803338032.8
0.012	424610.44	3338645.15	803331364.7
0.013	485232.43	3813330.28	803324696.6
0.014	566047.51	4445368.14	803318028.7
0.015	679161.3	5328544.1	803311360.9
0.016	848772.21	6649652.51	803304693.2
0.017	1131297.8	8841805.43	803298025.6
0.018	1695752.6	13190115.3	803291358.1
0.019	3384360.7	25954055.7	803284690.7
0.02	803278023	803278023	803278023.4

The result for the frequency output for iron, nickel and copper against the differential pressure is given in table 2

Table 2: Differential Pressure with Firon,, Fnickel and Fcopper

p	f Iron (Hz)	f nickel (Hz)	f copper (Hz)
0	169810504	1338107777	8.03411E+11
500	169956479	1339256386	8.03411E+11
1000	170102705	1340406968	8.03411E+11
1500	170249183	1341559528	8.03411E+11
2000	170395914	1342714072	8.03411E+11
2500	170542897	1343870606	8.03411E+11
3000	170690134	1345029133	8.03411E+11
3500	170837626	1346189660	8.03411E+11
4000	170985373	1347352191	8.03411E+11
4500	171133376	1348516731	8.0341E+11
5000	171281635	1349683286	8.0341E+11
5500	171430151	1350851862	8.0341E+11
6000	171578925	1352022462	8.0341E+11
6500	171727958	1353195094	8.0341E+11
7000	171877249	1354369761	8.0341E+11
7500	172026801	1355546469	8.0341E+11
8000	172176613	1356725224	8.0341E+11
8500	172326686	1357906030	8.0341E+11
9000	172477020	1359088894	8.03409E+11
9500	172627618	1360273820	8.03409E+11
10000	172778478	1361460815	8.03409E+11

The result of the Ton, T_{off}, time period, frequency, duty cycle with variation in resistance is given in table 3

Table 3: Variation with resistance with time period, duty cycle and frequency

ΔR	R_1	R_2	T on (s)	t off (s)	T total (s)	F (Hz)	DC
499	1	999	2.77893E-07	6.92307E-07	9.0159E-07	1109148	0.308224
400	100	900	3.465E-07	6.237E-07	9.009E-07	1110001	0.384615
300	200	800	4.158E-07	5.544E-07	9.009E-07	1110001	0.461538
200	300	700	4.851E-07	4.851E-07	9.009E-07	1110001	0.538462
100	400	600	5.544E-07	4.158E-07	9.009E-07	1110001	0.615385
0	500	500	6.237E-07	3.465E-07	9.009E-07	1110001	0.692308
-100	600	400	0.000000693	2.772E-07	9.009E-07	1110001	0.769231
-200	700	300	7.623E-07	2.079E-07	9.009E-07	1110001	0.846154
-300	800	200	8.316E-07	1.386E-07	9.009E-07	1110001	0.923077
-400	900	100	9.009E-07	6.93E-08	9.0159E-07	1109148	0.999231
-499	999	1	9.69507E-07	6.93E-10	9.6951E-07	1031452	1

The improved values with the following parameters is given in table 4 C= 1nF, R_1= 400 ohm, R_2= R_0-ΔR **R_0=500**, R_2= R_0+ΔR and R_2+ R_1= 1000 ohm

Table Error! No text of specified style in document.**: Improved values for micrometer measurement**

ΔR	R_1	R_2	t on (10^{-7}s)	t off (10^{-7}s)	T total (10^{-7}s)	F (Hz)	DC
499	1	999	5.6	13.2	18.8	531914.9	0.297872
400	100	900	6.6	11.8	18.4	543478.3	0.358696
300	200	800	7.5	11	18.5	540540.5	0.405405
200	300	700	8.5	9.8	18.3	546448.1	0.464481
100	400	600	9.6	8.6	18.2	549450.5	0.527473
0	500	500	10.7	7.4	18.1	552486.2	0.59116
-100	600	400	11.8	6.4	18.2	549450.5	0.648352
-200	700	300	13	5.3	18.3	546448.1	0.710383
-300	800	200	14.6	4.1	18.7	534759.4	0.780749
-400	900	100	16.4	3.1	19.5	512820.5	0.841026
-499	999	1	18.6	1.9	20.5	487804.9	0.907317

3.3 Frequency as a Function of Oscillations

Generally, vibrations in movement can be described or expressed by the following equations. In the case the seesaw bar shown above in Figure 2 through 4, we assume that the seesaw bar in the springs has a movement which is a simple harmonic motion according to the following equation;

$$X = 0.5l - o.5l \cos(2\pi f_s t) \quad (12)$$

The vibrations found in electronic circuit and in machines can be converted into useful frequencies as shown in equation 14 and 15.

$$f_1 = \frac{1.58\,Rl^2}{\mu_0 N^2 A(l+[0.5l-o.5l\cos(2\pi f_s t)](\mu_r-1))} \quad (13)$$

$$f_2 = \frac{1.58\,Rl^2}{\mu_0 N^2 A(\mu_r\, l+[0.5l-o.5l\cos(2\pi f_s t)](1-\mu_r))} \quad (14)$$

To check the effect of the sea saw bar frequency, equations [13], [14] and [15] are used. Assuming a coil of length of 20mm, number of turns = 100, cross sectional area A=pi(r*r) where r=1mm, an iron core with relative permeability 4728, and R= 1k ohm, then by changing the value of fs, the plots for the output frequency as a measure of x is obtained. Figure 8 shows the effect of the circuit as it oscillates, converting the deviations into these useful frequency values when the harmonics from the see-saw in the convulsion are given as 10Hz, 100Hz, 1000Hz and 10,000Hz respectively.

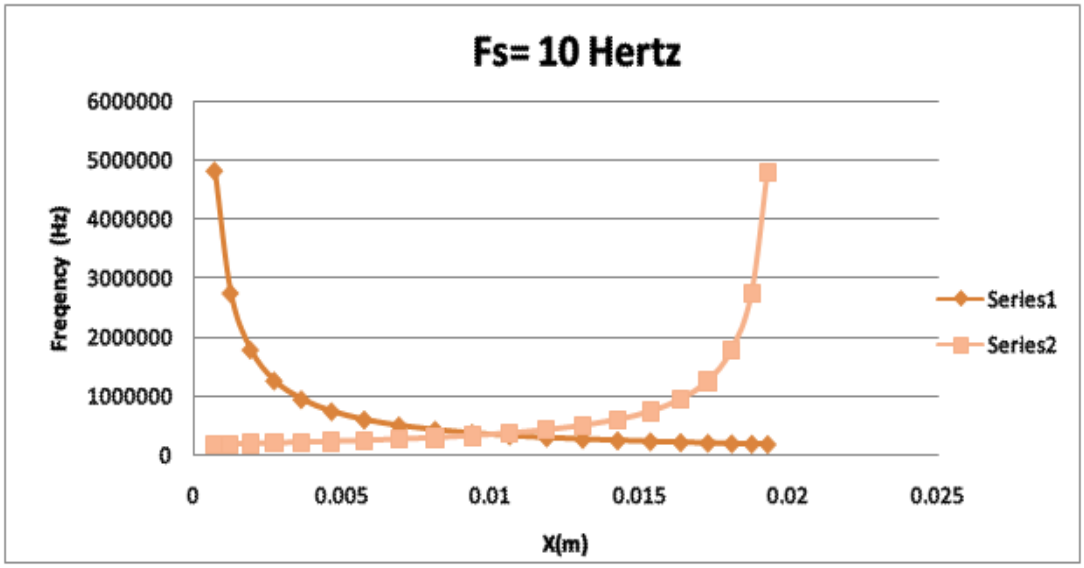

(a)

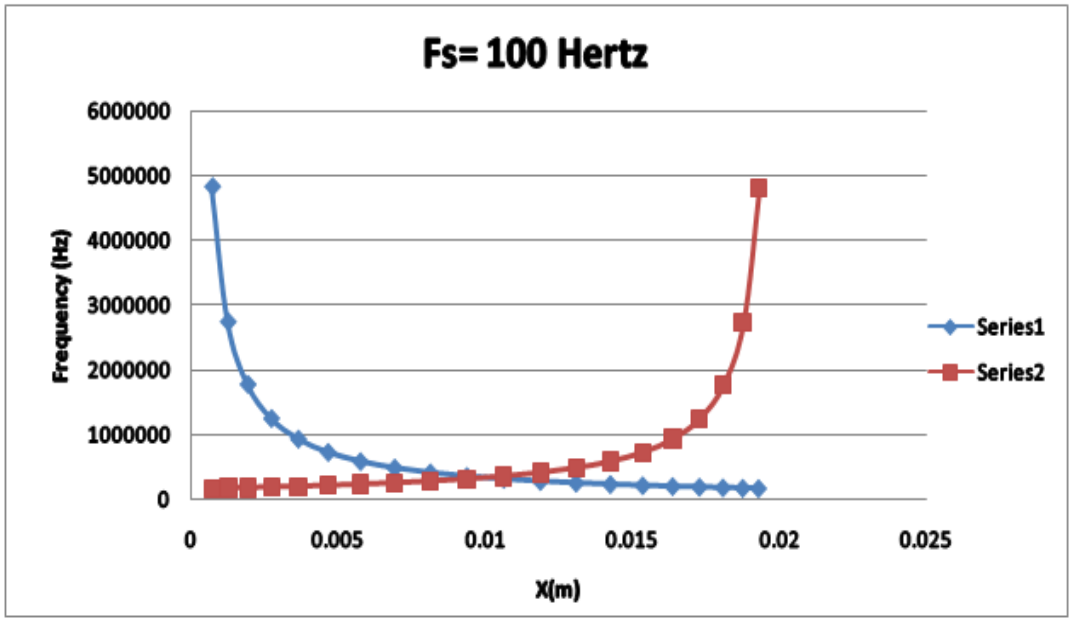

(b)

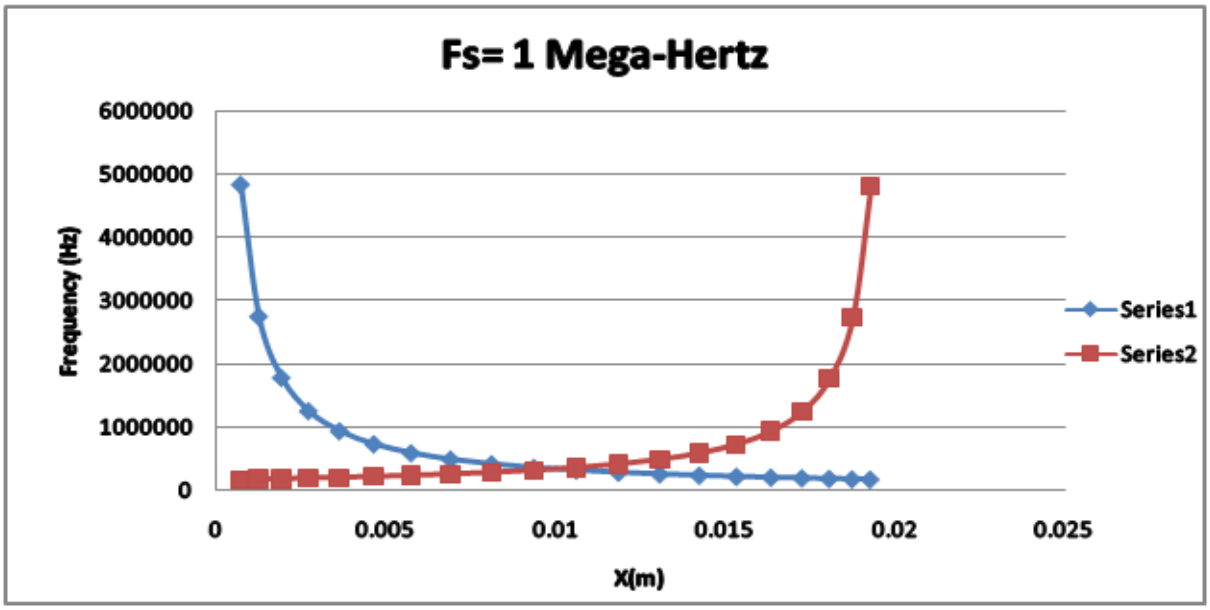

(c)

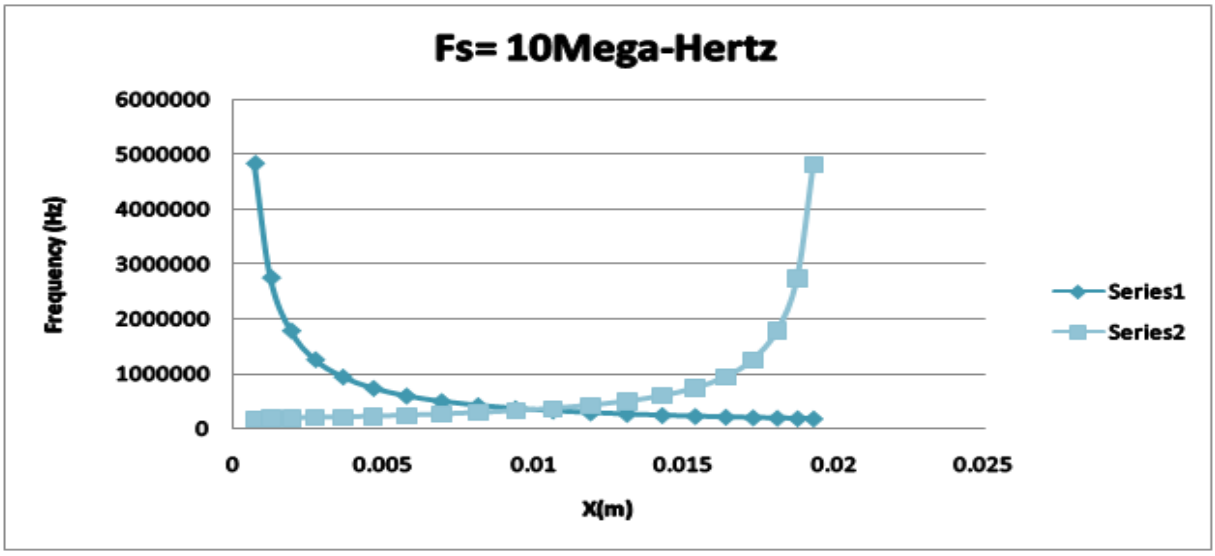

(d)

Figure 8: Plot of the Output Response for oscillating circuit for varying values of Fs.

4. Simulation Result and Analysis

A simulation of the designed mathematical model and its necessary derivations for frequency, frequency hysteresis, voltage and the current responses are carried out. The results obtained confirm the mathematical derivation plots with the simulation. Figure 9 (a) is the result of simulation of both circuits; the right and the left one using the same assumption that was used in the calculations. The green line represents the frequency output of the left side and the red one is for the circuit in the right-hand side as a measure of the core displacement.

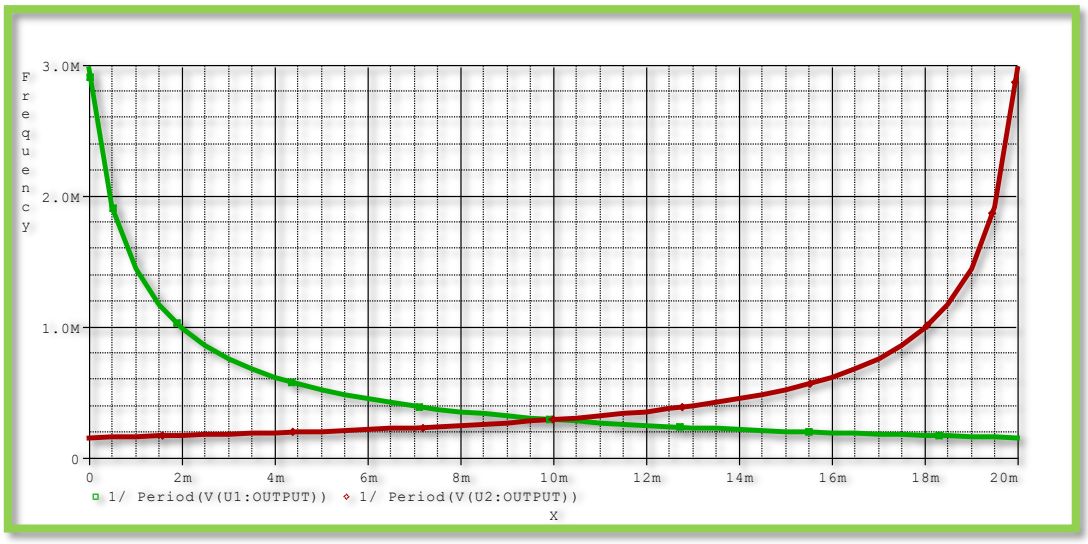

Figure 9 (a): A simulation of Frequency change in symmetrical variation with respect to core displacement.

Figure 9 (b) shows the output frequency when the sea saw frequency fs= 100 Hz, for **three** time periods, in every period, the displacement value change from 0 to l and from l to 0.

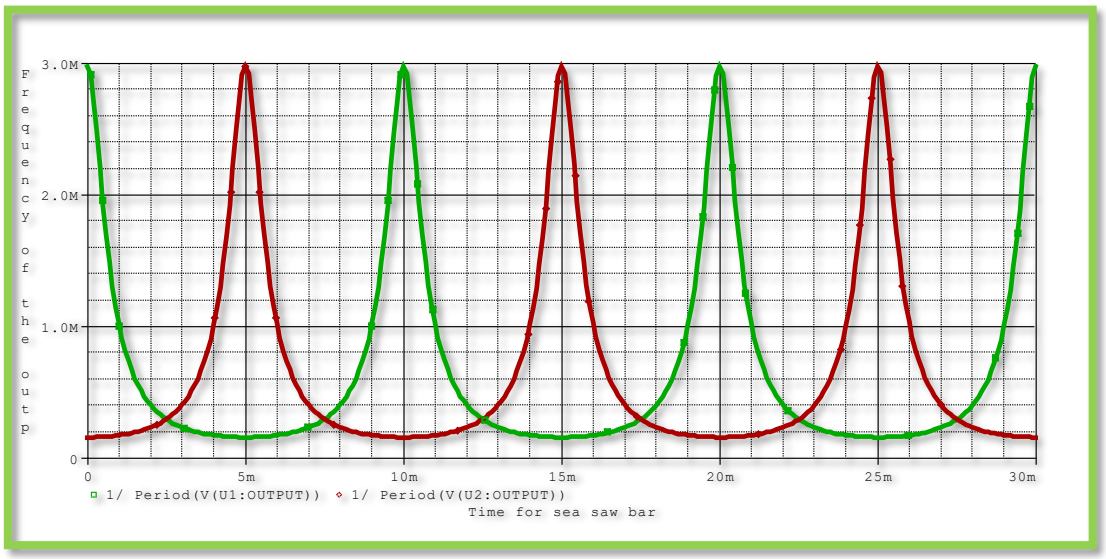

Fig.9 (b): Simulated Output for frequency with three time periods

Figure 10 (a)-(d) shows the result of simulation when the sea saw bar frequency is change. When the frequency of sea saw bar is 10Hz, x changes from 0 to l, and time t, is changed from 0 to 50ms, 0 to 100ms, 0 to 1000ms and 0 to 10000ms according to equation [15]. The results obtained confirm those of the derivations shown in section III of this work. A slight difference in simulation analytical deduction is due to the environmental effect on the circuit.

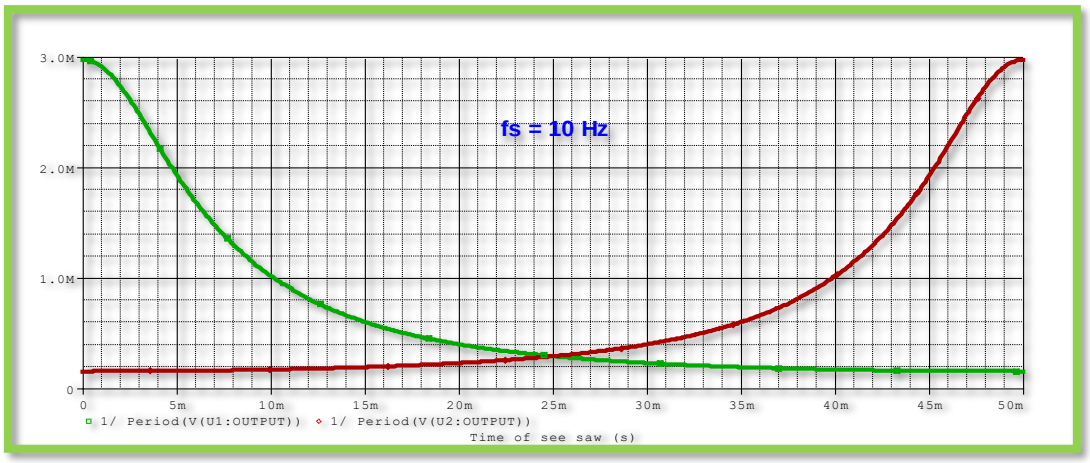
fs = 10 Hz
3.0M
2.0M
1.0M
0
0
5m
10m
15m
20m
25m
30m
35m
40m
45m
50m
1/ Period(V(U1:OUTPUT))
1/ Period(V(U2:OUTPUT))
Time of see saw (s)

(a)

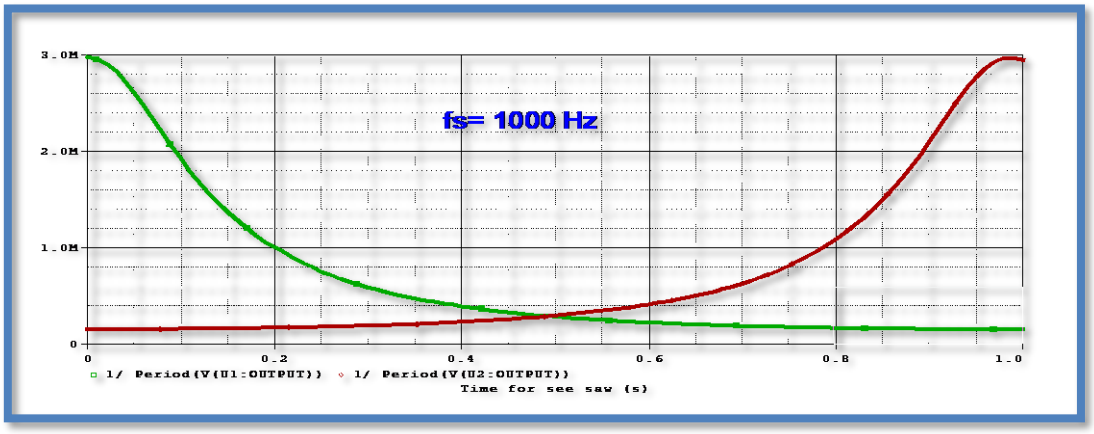
fs= 1000 Hz
3.0M
2.0M
1.0M
0
0
0.2
0.4
0.6
0.8
1.0
1/ Period(V(U1:OUTPUT))
1/ Period(V(U2:OUTPUT))
Time for see saw (s)

(b)

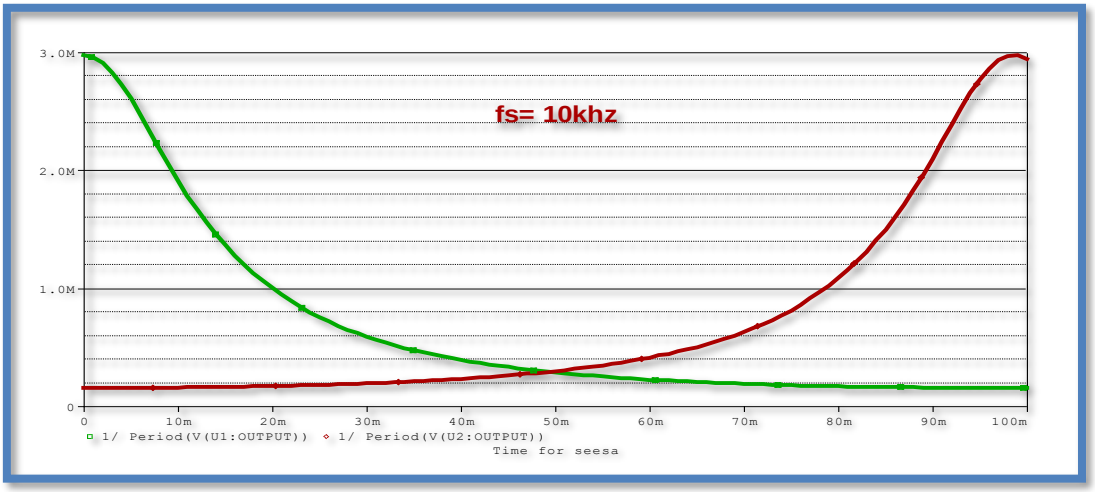
fs= 10khz
3.0M
2.0M
1.0M
0
0
10m
20m
30m
40m
50m
60m
70m
80m
90m
100m
1/ Period(V(U1:OUTPUT))
1/ Period(V(U2:OUTPUT))
Time for seesa

(c)

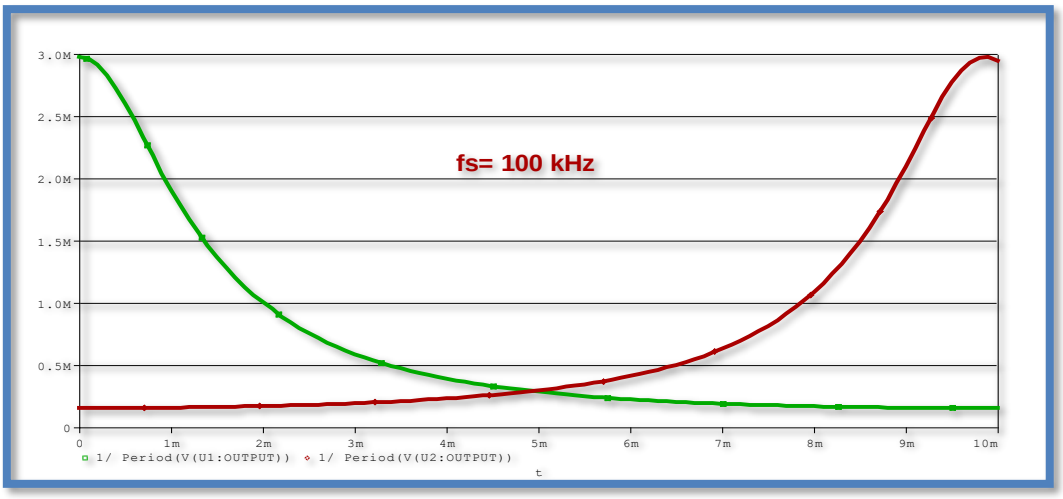

(d)

Figure 10 (a-d): Simulation values for different harmonics in the see-saw.

The table for the different frequencies giving rise to frequency hysteresis is given below in table 1. This table gives rise to Fig.6, showing the frequencies of the see-saw behavior when the core is differentially in and out of its coil as the circuit oscillate.

Table1: Simulation details of frequency hysteresis

X	delta f1	delta f2	delta f
0.001	0.109400729	8958.646289	4479.3778
0.002	1692127.847	18912.4638	855520.16
0.003	2257759.167	30037.02729	1143898.1
0.004	2540873.66	42551.79359	1291712.7
0.005	2710838.104	56734.72486	1383786.4
0.006	2824187.656	72943.17702	1448565.4
0.007	2905171.185	91644.4259	1498407.8
0.008	2965919.533	113461.451	1539690.5
0.009	3013174.592	139243.6828	1576209.1
0.01	3050982.636	170180.1802	1610581.4
0.011	3081919.134	207988.2244	1644953.7
0.012	3107701.365	255243.2833	1681472.3
0.013	3129518.39	315991.6318	1722755
0.014	3148219.639	396975.1606	1772597.4
0.015	3164428.091	510324.7128	1837376.4
0.016	3178611.023	680289.1565	1929450.1
0.017	3191125.789	963403.6494	2077264.7
0.018	3202250.353	1529034.969	2365642.7
0.019	3212204.17	3221162.707	3216683.4

A linear relationship exist between the inductance of the first coil, which increases when the core is moving in, while the core for the second coil is moving out, with decrease in inductance. The inductance change

ΔL is calculated and plotted in Figure 6. These inductances change leads to a frequency change and hysteresis for the output of the timers as seen from derivations and simulation results. This shows that the frequency is decreasing when the core is going in and increases when the core goes out.

At equilibrium state when the sea saw bar is horizontal, the displacement x is equal to half of the coil length, l and the value of the inductance for both coils is the same. This is clearly shown in Figure 6 at the point when x= 10mm, the inductance L=4.67mH for the two coils. The result of the inductance equality at this point is reflected to the frequency value as Figure 7.

The main difference between derivations and simulation result is seen when the coil is almost fully out. From derivation point, when the coil is fully out x=0, the frequency is larger than 800 Mega Hz, which is very large compared to other frequency values which ranges from 0.18 to 3.4 Mega Hz. On the other hand, simulation result shows that maximum frequency occurs when the core is fully out and this is at 3 MHz as shown Figure 7. Although, the result from derivations and simulation has shown that the sea saw bar frequency has no effect on the output frequency values, the frequency counter calculate the value which is equal to the time period of the timer output for every reading. So, if the sea saw frequency fs exceeds a certain value, the frequency counter will give wrong frequency output. This value is derived as shown in equation [16].

$$\sum_{x=0}^{x=l} 0.63 \frac{\mu_0 N^2 A}{Rl^2} (l + x(\mu_r - 1)) \quad (15)$$

5. Conclusion

Differential sensing system architecture is proposed as shown in Fig. 1 to Fig.4. This consists of two coils with varying cores in which a change in the core position will result in inductance change. These changes can be converted into frequency output in the processing part of the sensor using a timer circuit. Simulation of the proposed system shows a similar result with that of theoretical derivation. The sea saw bar frequency effect is checked and the limitation for this value. This was found in equation [16]. Finally, this novel design provides a platform for electro-mechanical and servomechanism system deviation in form of oscillation and vibration to be harvested into useful electrical signal by the help of designed differential inductive sensor using both coils transducers as shown in Fig. 3. The result obtained appears to be at minimum value of 0.001% of FSO which serve as improvement and introduction frequency hysteresis results in both derivations and in simulations.

REFERENCES

1. Mohamed A.S, Adel E.S and Soliman A.M., (2017) “A New Modeling Technique Based on Performance Data for Photovoltaic Modules and Horizontal Axis Wind Turbines” “A research Article on Wind Engineering and SAGE. (2017) 1-21.
2. Mohamed A.S and Soliman A.M., (2017) “ A novel study of using Oil Refinery Plants waste gases for Thermal Desalination and Electric Power Generation: Energy, exergy and Cost Evaluation” “Elsevier Journal on Applied Energy. 195 (2017) 453-477.
3. Ezzat, G. B., and H. M. Marvin Cheng, AUGUST 2011. “High-Sensitivity Inductive Pressure Sensor,” *IEEE Transactions On Instrumentation And Measurement*, VOL. 60, NO. 8,
4. Sahani, A. K.; Joseph, J.; Sivaprakasam, M., (2012). "Automated system for imageless evaluation of arterial compliance", *34th Annual International IEEE Conference on Engineering in Medicine and Biology Society (EMBC)*, pp.227- 231.

5. Grover, D. and Deller J. R., (1999). 'Digital Signal Processing And The Microcontroller, chapter 2, Motorola University Press - Prentice Hall Professional Technical Reference, Upper Saddle River, NJ. Pages 15-20
6. Hameed, S. A., Aboaba A., Khalifa A.A., Abdalla O.O., Daoud A.H., Saeed J.I., Mahmoud R.A., (2012) Framework for enhancement of image guided surgery: Finding area of tumor volume, Australian Journal of Basic and Applied Sciences, Volume 6, Issue 1, Pages 9-16, (ISI Cited publication)
7. Mohammed, S. S, George A. B., Vanajakshi L., and Venkatraman J., (2012). "A Multiple Inductive Loop Vehicle Detection System for Heterogeneous and Lane-Less Traffic," IEEE Transactions on Instrumentation and Measurement, Vol. 61, No. 5, 1353-1361.
8. Mohan, N. M., Shet A. R., Kedarnath S., and Kumar V. J., (2008). "Digital Converter for Differential Capacitive Sensors," IEEE TRANSACTIONS on Instrumentation and Measurement, Vol. 57, No. 11, pp.: 2576-2581.
9. Mohan, N. M., George A. B., and Kumar V. J., (2009). "Analysis of a Sigma–Delta Resistance-to-Digital Converter for Differential Resistive Sensors," IEEE Transactions on Instrumentation and Measurement, Vol. 58, NO. 5, 1617-1622
10. Ravindra W., (2006). 'Inductive Fiber-Meshed Strain and Displacement Transducers for Respiratory Measuring Systems and Motion Capturing Systems' IEEE Sensors Journal, Vol. 6, No. 3.
11. Saxena, S. C., and Sahu C., (1994). "Differential Inductive Ratio Transducer with Short-circuiting Ring for Displacement Measurement", IEEE Transactions On Instrumentation And Measurement, Vol. 43, NO. 5,
12. Slamwomir T., (2007). "Induction Coil Sensors-a review. Institute of Electrical Theory and Measurement", Ul Koszykowa 75,00-661 Warsaw, Poland, Pp 31-46.
13. Texas Instruments, "LM555 Data sheet" (2003).
14. Udaya K. M., and Duleepa J. T., (2011), "A Bidirectional Inductive Power Interface for Electric Vehicles in V2G Systems," IEEE TRANSACTIONS ON INDUSTRIAL ELECTRONICS, VOL. 58, NO. 10, pp. 4789-4796.
15. D. Abdulwahab, S. Khan, M. H Habaebi, (2023). " *Mathematical Differential Analysis of Atlantic Ocean Wind to Electrical Energy Generation in Lekki Peninsular Lagos Nigeria*", Journal of Electrical Electronics Engineering Research doi: 10.1109/ICOM.2011.5937149 vol. 85, no. 11, pp. 2720–2731.
16. D. Abdulwahab, S. Khan, J. Chebil and A. H. M. Z. Alam, "Symmetrical analysis and evaluation of Differential Resistive Sensor output with GSM/GPRS network," 2011 4th International Conference on Mechatronics (ICOM), Kuala Lumpur, Malaysia, 2011, pp. 1-6, doi: 10.1109/ICOM.2011.5937149.
17. D. Abdulwahab et al., "Identification of linearized regions of non-linear transducers responses," International Conference on Computer and Communication Engineering (ICCCE'10), Kuala Lumpur, 2010, pp. 1-4, doi: 10.1109/ICCCE.2010.5556753.
18. Deji A., Sheroz K, Musse M.A, Jalel C. (August 2014). Analysis and evaluation of differential inductive transducers for transforming physical parameters into usable output frequency signal August 2014 International Journal of the Physical Sciences 9(15):339-349 DOI:10.5897/IJPS12.655
19. Khan S., A. Deji, A.H.M Zahirul, J. Chebil, M.M Shobani, A.M Noreha. (Setember 2012)"Design of a Differential Sensor Circuit for Biomedical Implant Applications". *Australia. Journal of Basic and Applied. Sciences., 6(9): 1-9.* 10.1002/9781118329481.ch1.

Appendix I

Inductance of the part containing the core L_1 is given as:

$$L_1 = \frac{\mu_r \mu_0 N_1^2 A}{l-x} \qquad \text{(A-1)}$$

The inductance of the part with no core L_2 is given as:

$$L_2 = \frac{\mu_0 N_2^2 A}{x} \qquad \text{(A-2)}$$

The numbers of turns in the first and second inductors above the total number of the coil under consideration give by

$$N = N_1 + N_2 \qquad \text{(A-3)}$$

And, therefore, we know that

$$\frac{N_2}{N} = \frac{x}{l} N = \frac{Nx}{l}$$

Similarly;

$$N_1 = \frac{N(l-x)}{l} = N\left(1 - \frac{x}{l}\right) \qquad \text{(A-4)}$$

Substituting the values of N_1 and N_2 into equations above:

$$L_1 = \frac{\mu_r \mu_0 N^2 \left(1-\frac{x}{l}\right)^2 A}{l-x} = \frac{\mu_r \mu_0 N^2 A(l-x)}{l^2} \qquad \text{(A-5)}$$

$$L_2 = \frac{\mu_0 N^2 \left(\frac{x}{l}\right)^2 A}{x} = \frac{\mu_0 N^2 A x}{l^2} \qquad \text{(A-6)}$$

The total inductance is the series sum of the individual inductances L_1 and L_2, given as:

$$L = L_1 + L_2 \qquad \text{(A-7)}$$